Pergamon

Tetrahedron: *Asymmetry* 13 (2002) 1863–1873

TETRAHEDRON: *ASYMMETRY*

Computational study of the *syn*,*anti*-selective aldol additions of lithiated bis-lactim ether to 1,3-dioxolane-4-carboxaldehydes

María Ruiz, Vicente Ojea* and José M. Quintela

Departamento de Química Fundamental, Facultade de Ciencias, Universidade da Coruña, Campus da Zapateira, s/n, 15071 A Coruña, Spain

Received 19 June 2002; accepted 14 August 2002

Abstract—Ab initio (RHF/6-31G*) and two-layer hybrid ab initio:semi-empirical (ONIOM) calculations were carried out to investigate the *syn*,*anti*-selective aldol additions of lithiated Schöllkopf's bis-lactim ether to 1,3-dioxolane-4-carboxaldehydes. Initial lithium–carbonyl coordination to form a disolvated complex with 4.6–8.4 kcal/mol exothermicity is followed by the rate-determining reorganization to the aldolate products through six-membered chair-like transition structures. The experimental stereoselectivities of the aldol additions have been adequately reproduced. According to the calculations, the most stable transition structures are characterized by a non-Anh conformation of the aldehyde moiety. In addition, the β-methyl substituent of the aldehyde, *trans* to the carbonyl group, is found to increase the energy barrier of the competitive pathways, thus reinforcing the *syn*,*anti*-stereoselection of the aldol process.

1. Introduction

Optically active β-hydroxy-α-amino acids are versatile synthons that may be employed in the construction of a wide variety of nitrogen-containing natural products. One classic route for the stereocontrolled synthesis of β-hydroxy-α-amino acid derivatives involves aldol reactions of chiral glycine equivalents. Among several classes of readily available chiral glycine enolates,[1] Schöllkopf's bis-lactim ether azaenolates have proven to be highly diastereoselective in aldol processes,[2] particularly in double stereodifferentiating reactions with α-alkoxyaldehydes. Using the appropriate metal counterpart, reactions of bis-lactim ethers with either matched or mismatched cyclohexylidene glyceraldehyde and α,β-*syn*-dihydroxy aldehydes proceed under almost complete azaenolate control, affording the *syn*-adducts with excellent diastereoselectivities.[3,4] Thus, our convergent route to fucosamines **1a**–**c** (see Scheme 1) relied on elaboration of the polyhydroxy amino acid precursor **2** that can be directly accessed by the highly *syn*-selective aldol reaction of lithiated Schöllkopf's bis-lactim ether **3** and 1,3-dioxolane-4-carboxaldehyde **4**.[5,6]

In spite of the effort devoted to the synthesis of non-proteinogenic amino acids using Schöllkopf's methodology, the mechanistic basis for the reactions of metalated bis-lactim ethers has not yet been firmly established. In particular, the factors that determine the diastereofacial discrimination in aldol reactions of bis-lactim ethers with chiral aldehydes are not well understood. Schöllkopf and co-workers invoked the Zimmerman–Traxler transition state model,[7] and proposed idealized chair-like structures which minimize the steric interactions between the bis-lactim moiety and the equatorial aldehyde substituents to qualitatively account for the selective formation of *trans*,*syn*-adducts.[2e,g,h] The higher *trans*,*syn*,*anti*-selectivity observed in the additions to matched α-alkoxyaldehydes was understood in terms of a combination of such transition state model with the Felkin–Anh model[8] for 1,2-asymmetric induction.[3] Following Schöllkopf's

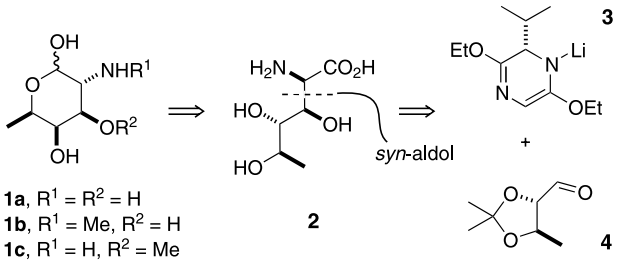

Scheme 1. Synthesis of D-fucosamines.

* Corresponding author. Tel.: +34-981167000; fax: +34-981167065; e-mail: ojea@udc.es

0957-4166/02/$ - see front matter
PII: S0957-4166(02)00479-2

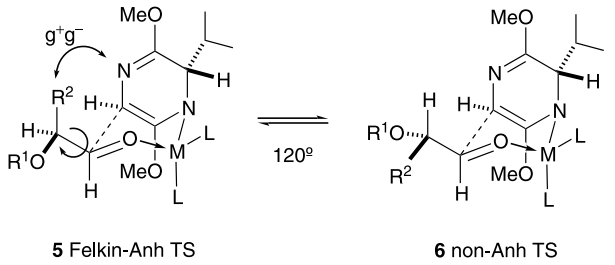

5 Felkin-Anh TS **6** non-Anh TS

Scheme 2. Idealized transition structures for the aldol addition.

rationalization, the chair-like/Felkin–Anh transition structure **5**, with an anticlinal disposition of the α-hydrogen atom with respect to the carbonyl group and the developing carbon–carbon bond antiperiplanar to the α-alkoxy substituent (see Scheme 2), would be further stabilized relative to the diastereomeric transition states.

Nevertheless, as was first stressed by Roush in his analysis of the stereoselectivity in the additions of *Z*(*O*)-enolates to α-methyl chiral aldehydes,[9] transition structure **5** would be destabilized by the presence of a g^+g^- double gauche pentane interaction between one of the bis-lactim nitrogen atoms and the R^2 group on the α-carbon of the aldehyde. This unfavorable steric interaction raises the energy of the Felkin–Anh pathway and other transition structures, also leading to the major *trans*,*syn*,*anti*-adduct, may become important. Among the possible ways for relaxing this *syn*-pentane interaction, a 120° rotation around the O=C–C(α) single bond gives rise to the 'non-Anh'[10] transition structure **6**, characterized by an anticlinal relationship between α-alkoxy and carbonyl groups and less serious gauche interactions eclipsing hydrogen atoms of the reaction partners.

The relative contribution of the Felkin–Anh, non-Anh and other diastereomeric transition states to the reaction pathway will depend on the particular nature of the substituents on the α-carbon of the aldehyde (R^1 and R^2), and can not be intuitively assessed. Thus, to gain more quantitative insight into the stereocontrol elements determining the π-facial selectivity and verify whether a closed transition state model combined with the Felkin–Anh or the non-Anh hypothesis could indeed rationalize the stereochemical course of these aldol additions, we have performed a detailed theoretical study of the possible reaction pathways associated with the aforementioned process. Thus, in this paper we introduce an inexpensive computational approach for the analyses of the sense and degree of stereoselection in the double stereodifferentiating aldol additions of metalated bis-lactim ethers, that could result in a useful tool for the prediction of the scope and limitations of such processes in the stereocontroled synthesis of β-hydroxy-α-amino acid derivatives.

2. Selection of models and methods

By analogy with previous theoretical studies on kinetically controlled aldol additions,[11–18] the reaction between the lithium azaenolate **3** and the dioxolanecarboxaldehyde **4** should involve an initial coordination of the carbonyl oxygen to the lithium atom to form the complex **7** (see Scheme 3). Subsequently, reorganization of this intermediate through competing six-membered transition structures would afford mixtures of the lithium aldolates 3,6-*trans*-3,1′-*syn*-1′,2′-*anti*-**8**, 3,6-*trans*-3,1′-*anti*-1′,2′-*syn*-**9**, 3,6-*cis*-3,1′-*anti*-1′,2′-*anti*-**10**, and 3,6-*cis*-3,1′-*syn*-1′,2′-*syn*-**11**. Since low reagent concentration and high solvent concentration will promote reaction via the more highly solvated and less aggregated species,[19] complete dissociation of the possible oligomeric clusters was assumed in the present study by considering discrete solvation of the lithium with an adequate number of THF molecules.[20,21]

Computational studies using Hartree–Fock (HF)[22] and density functional theory (DFT)[23] with standard basis sets (3-21G, 6-31G* and 6-31+G*) have contributed significantly toward a better understanding of organolithium compounds, and in particular those with N–Li and O–Li bonds.[24] However, the use of high-level ab initio calculations for large synthetic problems like **7**–**11u**–**t** is well-known to be computationally expensive, due to the presence of multiple rotatable bonds that make extensive conformational analyses along the reaction coordinate necessary. High-level ab initio treatment of such problems could only be handled on a 'small' model, excluding the electronic and steric effects

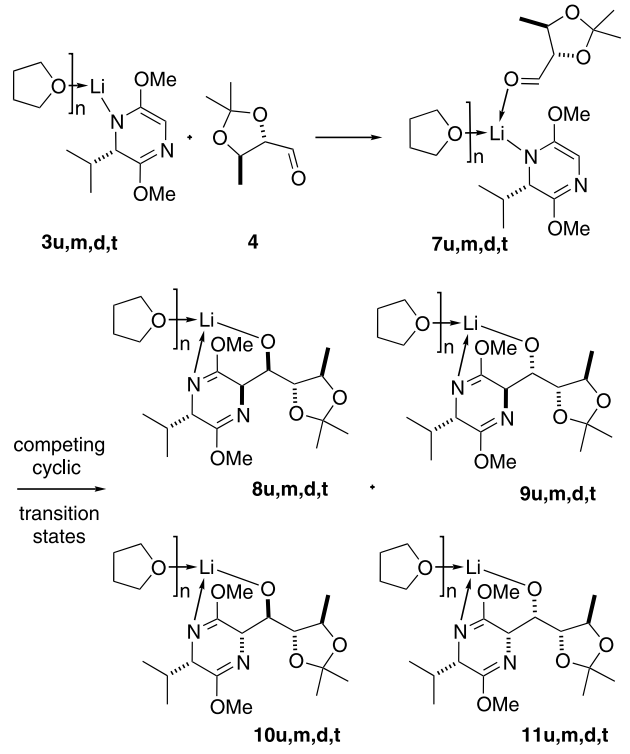

Scheme 3. Proposed mechanism for the addition of **3** to **4** in THF. Legend: **u**, $n=0$; **m**, $n=1$; **d**, $n=2$; **t**, $n=3$.

from parts of the system, while calculations on the complete or 'real' model would be practical only at a low level of theory, also compromising the reliability of the results. For the theoretical description of the present problem we thought that the best compromise between accuracy and speed would be achieved by using hybrid methods, considering the system divided into several regions, each of them with a different computational description. Thus, for the study of the aldol reaction between **3u–t** and **4** we have utilized the ONIOM method developed by Morokuma et al.,[25] which has been proven to be a very valuable tool for the theoretical treatment of large molecular systems.[26] Within this extrapolation method we considered a two layer scheme (ab initio:semi-empirical) for the partition of the system, as depicted in Fig. 1.[27]

The ab initio description was limited to an 'inner layer' including the critical parts of the reacting system: the atoms directly involved in the breaking and forming bonds and other areas sensitive to electronic effects, such as the groups directly bonded to the azaenolate moiety and to the α position of the aldehyde as well as the oxygen atoms of the solvent molecules coordinated to lithium. Thus, by replacing the groups excluded from the inner layer with hydrogen atoms, the ab initio model was reduced to the interaction of a lithiated dihydropyrazinone and (2*S*)-hydroxypropanal in the presence of water molecules, which has been treated in this work at the HF level using the 3-21G* and 6-31G* basis sets.[28]

For the low-level treatment of the entire system,[29] where the steric and electrostatic influence of the 'outer layer' is evaluated, we have employed the semi-empirical MNDO method.[30] In spite of its well known shortcomings,[31] MNDO has been shown to successfully reproduce Li–N and Li–O interactions by comparisons with experimental results and ab initio calculations.[32] Thus, MNDO method's capacity to calculate geometries of chemically realistic reactants and transition structures bearing a full complement of alkyl substituents and solvent has been clearly established for organolithium compounds in general and for lithium amides and enolates in particular.[33] Thus, ONIOM calculations were performed with the (HF/3-21G*:MNDO) basis set during the initial conformational searches and with the (HF/6-31G*:MNDO) basis set for the reoptimization of all located stationary points. These basis sets will be referred to as (I) and (II), respectively, throughout this paper. Although the calculated MNDO energies are usually not as accurate as the MNDO geometries, it has been shown that for lithium compounds the use of MNDO geometries followed by single point ab initio energy evaluations yields a potential energy surface which reproduces all the qualitative features of the fully ab initio surface.[34] Therefore, we have also computed B3LYP/6-31+G* energies on the most significative ONIOM geometries.

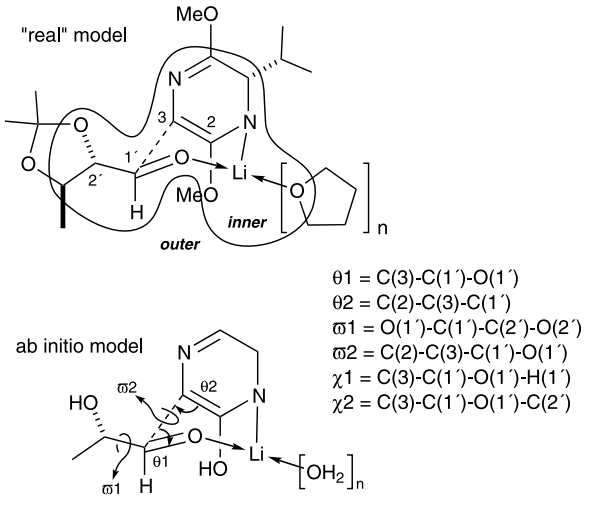

Figure 1. High level (ab initio) and low level (semi-empirical) layers for the ONIOM extrapolation, with angle definitions.

The reliability of the method combination and of the partition applied to the system were also evaluated through additional ab initio calculations on the complete model. As accurate structures have been calculated for solvated lithium amides at the HF/6-31G* level, and only small variations were observed with respect to the geometries optimized at the more time-consuming B3LYP/6-31+G* level,[35] the most significant ONIOM geometries were finally computed at the B3LYP/6-31+G*//HF/6-31G* level.

3. Computational results and discussion

3.1. Intermediate complexes

In the gas phase, addition of azaenolates **3u**, **3m** or **3d** to dioxolanecarboxaldehyde **4** proceeds first by the exothermic formation of the lithium-coordinated complexes **7u–d** shown in Scheme 4. These complexes are formed with no apparent reaction barriers. It is likely that in solution this coordination proceeds by replacement of a solvent molecule from the solvated azaenolate. Most stable conformations found for the complexes show the lithium atom above the plane of the pyrazine ring, providing a *trans* disposition between the lithium-coordinated carboxaldehyde and the isopropyl group. The complexation with lithium promotes a longer C=O bond distance, thus yielding a more electrophilic carbonyl carbon. In this manner, the O–C distances in the solvated or unsolvated complexes are calculated between 0.003 and 0.019 Å larger than in the aldehyde **4**. The lowest energy conformations located for the unsolvated complex **7u** at ONIOM(I) and HF/6-31G* levels are characterized by a four-coordinated cation, due to the interaction of the lithium with the nitrogen and the vicinal methoxy group of the azaenolate and with both the carbonyl and α-alkoxy oxygens of the aldehyde. The conformational analyses of the mono and disolvated complexes, **7m** and **7d**, are dominated by rotamers where the carbonyl group shows isoclinal and antiperiplanar relationships with the β-carbon atom and the α-alkoxy group, respectively.

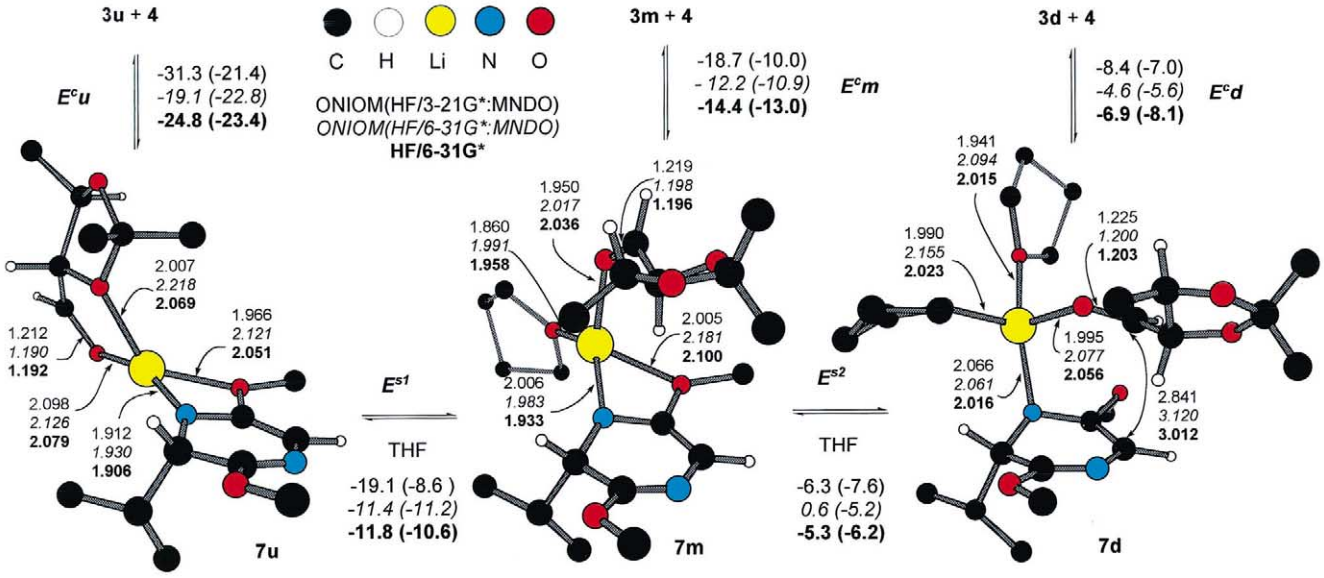

Scheme 4. Solvation equilibria for the intermediate complex **7**. Optimized distances, complexation energies ($E^c u$, $E^c m$ and $E^c d$), first and second solvation energies (E^{s1} and E^{s2}) calculated at ONIOM(I) (in plain text), ONIOM(II) (in italics), and HF/6-31G* (in bold) and relative single-point energies computed at the B3LYP/6-31+G* (in parentheses) are in Å and kcal/mol, respectively. Hydrogen atoms are omitted, except for the chiral and prochiral centers.

At all of the levels studied, specific solvation has some influence upon the structure of the intermediate complexes. The unsolvated (**7u**) and monosolvated (**7m**) complexes maintain the coordination between lithium and vicinal methoxy group, already shown by the parent azaenolates **3u** and **3m**. This interaction is not present in the disolvated complexes **7d**. Lithium coordination requirements in the intermediate complexes are satisfied with only two solvent molecules, and the interaction with the vicinal methoxy group is no longer necessary. Disolvated species also differ from the unsolvated and monosolvated ones by the geometry of the complexation. Only the disolvated complexes adopt a 'transition-state-like' geometry where a conformationally well-oriented approximation of the aldehyde and azaenolate partners enables the facing of their π-systems with less than 3.13 Å of separation between the reacting carbon centers.[36]

The addition of the first solvent molecule is the most effective, stabilizing the intermediate complex by more than 8.6 kcal/mol, while the introduction of the second one reduces the energy of the systems by less than 7.6 kcal/mol. Because of the reduced freedom of motion each solvation process should also be unfavorable entropically, and the saturation of the lithium center on the azaenolate–aldehyde complexes by coordination to solvent is not necessarily a thermodynamically favored process. Thus, in addition to the disolvated complexes, with the lowest energy, monosolvated species may also be important intermediates in the reaction pathway. In this way, we decided to analyze all possible rearrangements, considering both the monosolvated and the disolvated lithium-coordinated complexes **7m** and **7d**.

3.2. Monosolvated transition structures

The reorganization of the intermediate complexes must enable the formation of a single bond between two prochiral centers, and thus, four different topologies can be present in the corresponding transition states. In this manner, four different reaction pathways (a consequence of the interaction of each of the faces of the α-carbon atom of the azaenolate and the carbonyl carbon of the aldehyde), were considered. The (*Re*:*Re*), (*Re*:*Si*), (*Si*:*Si*) and (*Si*:*Re*) interactions, giving rise to transition states with 3,6-*trans*-3,1′-*syn*-1′,2′-*anti*, 3,6-*trans*-3,1′-*anti*-1′,2′-*syn*, 3,6-*cis*-3,1′-*syn*-1′,2′-*syn* and 3,6-*cis*-3,1′-*anti*-1′,2′-*anti* configurations were designated as the ***tsa***, ***tas***, ***css*** and ***caa*** reaction pathways, respectively.

At the ONIOM(I) level, full optimization of the selected starting geometries (see the computational details) in the monosolvated reaction channel enabled the location of seventeen different transition structures. In the ***tsa*** pathway, four different conformers were found within an energy interval of 1.3 kcal/mol. The ***tas***, ***css*** and ***caa*** families of transition structures were constituted by five, six and two conformers, that were calculated to be higher in energy than the most stable member of the ***tsa*** pathway, in agreement with the experimental results.[37] Most stable conformers located for each of the diastereomeric reaction pathways were reoptimized at the ONIOM(II) and HF/6-31G* levels, giving rise, in all the cases, to the chair-like structures **pro-8m** and **pro-10m** and the half-chair-like structures **pro-9m** and **pro-11m** depicted in Fig. 2.

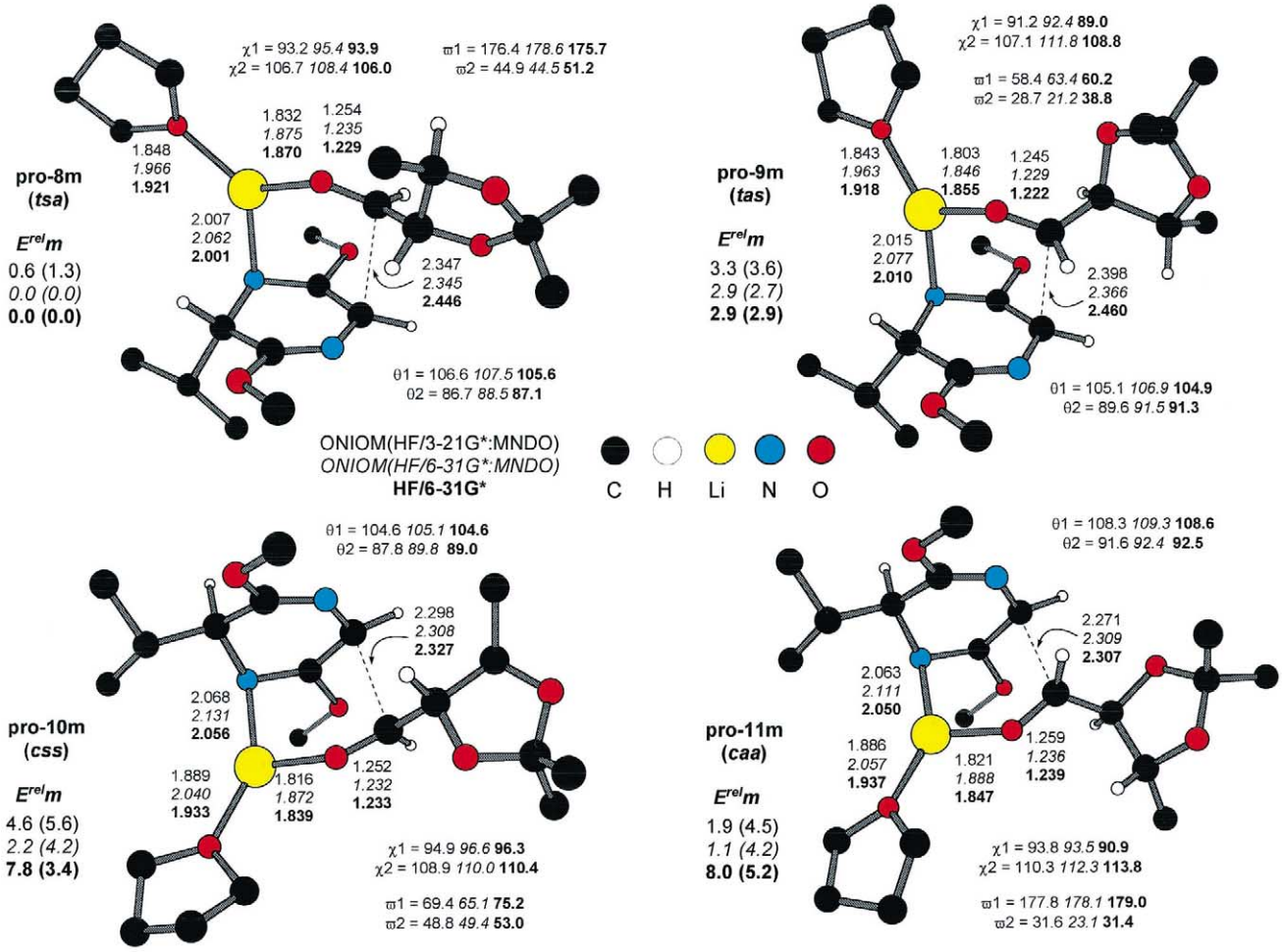

Figure 2. Optimized distances (in Å), angles (in °) and relative energies (in the monosolvated reaction channel, $E^{rel}m$) calculated at ONIOM(I) (in plain text), ONIOM(II) (in italics), and HF/6-31G* (in bold) levels for transition structures **pro-8**–**11m**. Relative single-point energies computed at the B3LYP/6-31+G* level are in parentheses. All energies are in kcal/mol. Hydrogen atoms are omitted, except for the chiral and prochiral centers.

The most stable monosolvated transition structures located in the ***caa*** and ***css*** pathways at the ONIOM(I) level, and in any diastereomeric pathway at the ONIOM(II) and HF/6-31G* levels, showed a trigonal planar coordination of the lithium cation. In the monosolvated transition structures the attack angles of the azaenolate on the aldehyde moiety are close to tetrahedral (θ1 between 104 and 110°), whereas the electrophilic attack angles on the azaenolate are isoclinal, with slightly lower values in the ***tsa*** and ***css*** pathways (θ2 between 86 and 89°) than in the ***tas*** and ***caa*** ones (θ2 between 89 and 93°). In the chair-like transition structures, with C(3)–C(1′) distances between 2.27 and 2.46 Å, non-bonding interactions between the pyrazine ring and the aldehyde substituent deviate the nucleophilic attack trajectory from the normal plane that bisects the pyramidalized carbonyl carbon. Thus, the torsional angles χ1 and χ2, that were proposed by Houk[11d] to describe the 'Flippin–Lodge angle',[38] were calculated in the intervals 88–97 and 106–114°, respectively.

The conformations of the monosolvated transition structures were found to be dependent on their relative configuration. Transition structures **pro-8m** and **pro-10m**, with *lk* topology, showed lower distortions from the idealized chair-like geometries than **pro-9m** and **pro-11m**, with an *ul* topology. Vicinal interactions of the α-substituents of the aldehyde moiety result more demanding in the *ul* series than in the *lk* series, as they involve the methoxy group instead of the nitrogen lone pair of the bis-lactim ring. Thus, these interactions may be responsible for the reduction of the ϖ2 dihedral and the preference for half-chair-like conformations showed by **pro-9m** and **pro-11m**. Conformational preferences of the aldehyde moiety in the monosolvated transition structures were found also dependent on the relative configuration at positions 1′ and 2′. At all the levels studied the transition structures **pro-8m** and **pro-11m**, characterized by a 1′,2′-*anti* topology consequence of the interaction with the *Re* face of the carbonyl moiety, showed an antiperiplanar relationship between the carbonyl and the α-alkoxy groups (ϖ1 between 175 and

179°) or 'non-Ahn conformation'. Conversely, the transition structures **pro-9m** and **pro-10m**, derived from the interaction with the *Si* face of the carbonyl moiety and characterized by a 1′,2′-*syn* topology, showed a synclinal disposition of the carbonyl and the α-alkoxy groups (ϖ1 between 58 and 76°) or 'Ahn conformation'.

3.3. Disolvated transition structures

The analysis of the rearrangement of the disolvated intermediate complex **7d** at the ONIOM(I) level led to the location of 14 different transition structures. In agreement with the experimental results, the most stable transition structures were found in the ***tsa*** pathway, grouped in two families of chair-like conformations characterized by either an antiperiplanar or synperiplanar disposition of the carbonyl and α-alkoxy groups. The ***tas*** family, constituted by six members with chair-, half-chair- or boat-like geometries, was found more than 3 kcal/mol higher in energy. A similar study of the ***css*** and ***caa*** pathways enabled the location of other four transition structures, which were determined more than 9 kcal/mol higher in energy than the most stable conformation in the ***tsa*** family. Reoptimization at the ONIOM(II) and HF/6-31G* levels gave rise to the chair-like conformations **pro-8d** and **pro-10d**, and the half-chair-like ones **pro-9d** and **pro-11d**, represented in Fig. 3, as the most stable transition structures in each of the diastereomeric reaction pathways.

All the disolvated transition structures **pro-8-11d** show a tetrahedral environment for the lithium cation and, as previously determined for the monosolvated series, they are characterized by C(3)–C(1′) bond forming lengths between 2.23 and 2.46 Å, tetrahedral nucleophilic attack angles (θ1 between 104 and 110°), isoclinal electrophilic attack angles (θ2 between 86 and 94°), and clear 'Flippin–Lodge' deviations of the nucleophilic attack trajectory, with χ1 and χ2 dihedrals in the intervals 89–98 and 104–115°, respectively.

The conformations of the disolvated transition structures were also found to be dependent on their relative configuration. Thus, 1′,2′-*anti* transition structures **pro-8d** and **pro-11d**, derived from the interaction of the

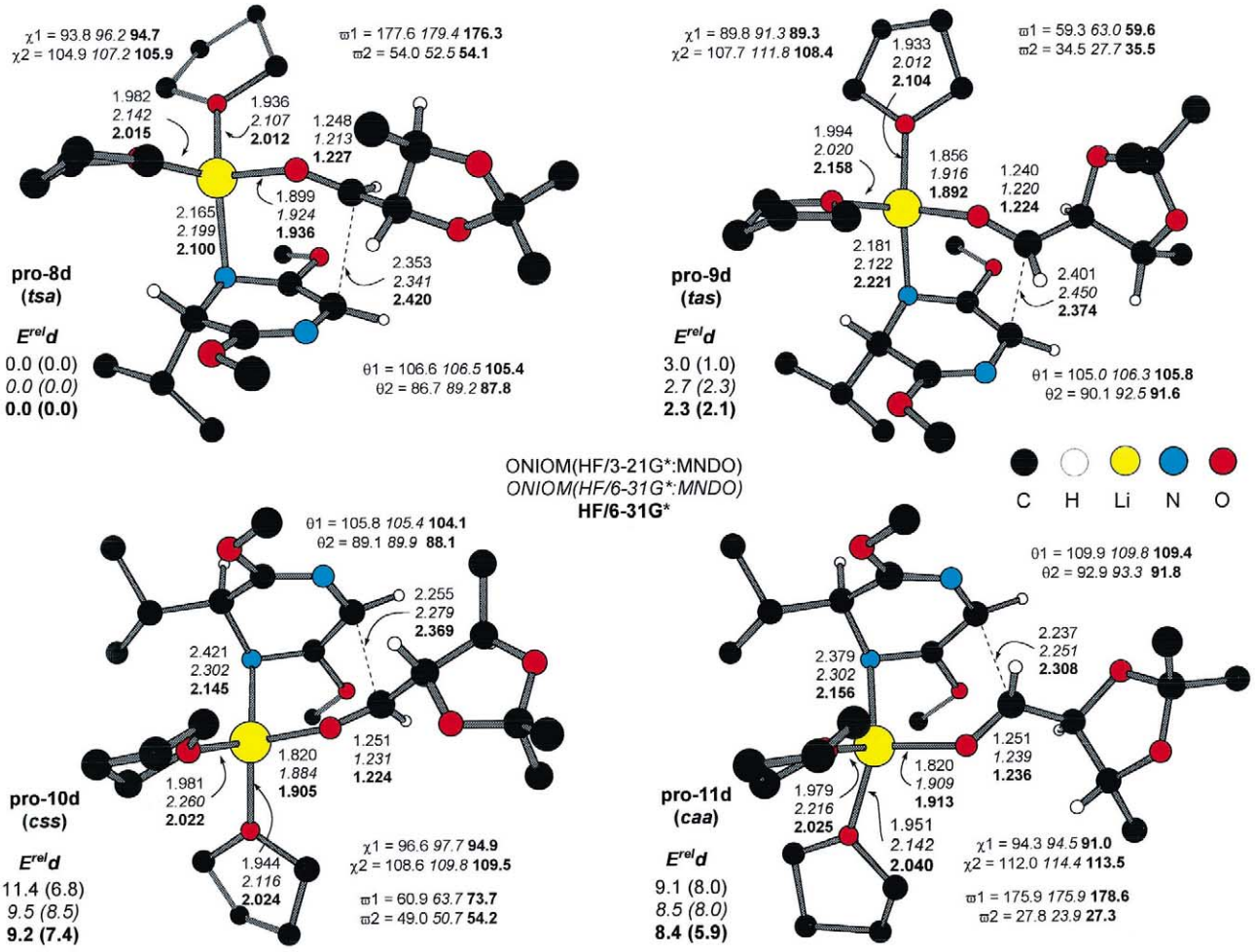

Figure 3. Optimized distances (in Å), angles (in °) and relative energies (in the disolvated reaction channel, $E^{rel}d$) calculated at ONIOM(I) (in plain text), ONIOM(II) (in italics), and HF/6-31G* (in bold) levels for transition structures **pro-8–11d**. Relative single-point energies computed at the B3LYP/6-31+G* level are in parentheses. All energies are in kcal/mol. Hydrogen atoms are omitted, except for the chiral and prochiral centers.

azaenolate with the *Re* face of the carbonyl group, showed a non-Ahn conformation (ϖ1 between 175 and 180°), while the 1′,2′-*syn* transition structures **pro-9d** and **pro-10d**, arising from the interaction with the *Si* face of the carbonyl group, showed synclinal dispositions of the carbonyl and the α-alkoxy groups (ϖ1 between 59 and 74°). In addition, for the transition structures with *lk* topology, **pro-8d** and **pro-10d**, only small deviations from the prototypical chair-like dihedrals were determined (ϖ2 dihedral between 49 and 55°), while the transition structures **pro-9d** and **pro-11d**, characterized by the *ul* topology, showed ϖ2 dihedrals between 24 and 36°, determining half-chair-like geometries.

3.4. Activation energies and reaction channels

Accordingly to the ratio of the differences between the C(1′)–O(1′) bond lengths in the intermediate complexes, the transition structures and the aldolate products, the monosolvated transition structures **pro-8–11m** and the disolvated transition structures **pro-8–11d** are estimated[39] to be 15–24 and 9–16%, respectively, along the reaction coordinate. In agreement with this early character for the transition states in both reaction channels, the activation energies for aldolate formation are computed to be only slightly positive. The activation barriers, corresponding to the progress of the reaction through the lowest energy ***tsa*** transition structures, calculated at the ONIOM(I), ONIOM(II) and HF/6-31G* levels are of 5.9, 6.4 and 7.0 kcal mol^{-1}, respectively, in the monosolvated channel, and of 0.7, 4.1 and 1.8 kcal/mol, respectively, in the disolvated channel.[40] Thus, the reaction channels involving disolvated intermediate complexes and disolvated transition structures seem to be favored at all the levels of theory over those with participation of the monosolvated species.

From the examination of the located transition structures it appears that calculated models are in agreement with the qualitative model proposed by Roush to explain the stereochemical course of the aldol additions of *Z*(*O*)-enolates.[9] Thus, at all the levels studied, the calculated transition structures in the ***tsa*** reaction pathway, which gives rise to the major aldolate product, are chair-like and show a non-Anh conformation which minimizes the g^+g^- double gauche pentane interactions between the bis-lactim and the aldehyde substituents. In fact, only two transition structures could be located in the ***tsa*** family with Felkin–Anh conformations, and they resulted 2.3 and 3.6 kcal/mol higher in energy, respectively, than the corresponding non-Anh conformations.

The activation energies were found to be substantially dependent on the level of calculation. When electron correlation is included to some extent by performing single-point energy calculations at the B3LYP/6-31+G* level, the most stable mono and disolvated transition structures are calculated to be lower in energy than the corresponding chelated complexes (**7m** and **7d**), indicating direct conversion of the intermediates into the aldol products, without any energy barrier. Nevertheless, the values of the transition-state relative energies computed at such level on the geometries optimized at the ONIOM(II) and HF/6-31G* levels conveniently reproduce the sense and degree of the stereoselection in the aldol addition. Negative activation energies have been previously computed at the MP2/6-31G*//RHF/3-21G and MP2/6-31G*//RHF/6-31G* levels for the aldol addition of formaldehyde to the lithium enolate derived from acetaldehyde.[11b]

3.5. Influence of β-substituent

General models acknowledging the influence of β-substituents on the facial selectivity in nucleophilic additions to the carbonyl group are not yet well developed. Therefore, to gain more insight into the possible role of the β-methyl substituent of the aldehyde as a third stereochemical determinant of the aldol addition, we decided to extend our computational analysis and model the reaction of the azaenolate **3** with the unsubstituted 1,3-dioxolane-4-carboxaldehyde.

After replacing the β-methyl group with a hydrogen atom in all the significant stationary points located in the disolvated reaction channel, reoptimization at the ONIOM(I), ONIOM(II) and HF/6-31G* levels led to the corresponding sets of β-unsubstituted intermediate complexes and transition structures. The geometries calculated for the most stable β-unsubstituted models were found to be very similar to those previously obtained in the β-Me-substituted series (see **7H**, **pro-8H** and **pro-9H**, in Fig. 4). Comparison of the heavy atom positions for the couples of β-unsubstituted and β-Me-substituted intermediate complexes (**7d**/**7H**) and transition structures in the ***tsa*** and ***tas*** series (**pro-8d**/**pro-8H** and **pro-9d**/**pro-9H**) resulted in RMS deviations of less than 0.143, 0.119 and 0.157 Å, respectively.

In the β-unsubstituted series, as previously found for the β-Me-substituted series, all levels of theory indicated a kinetic preference for the non-Anh, chair-like transition structures of the ***tsa*** reaction pathway. The most stable β-unsubstituted transition structures (**pro-8H**) required activation energies of 1.4, 4.3 and 1.8 kcal/mol at the ONIOM(I), ONIOM(II) and HF/6-31G* levels, respectively, which are very similar to those previously computed for the β-Me-substituted analogues. Nevertheless, the activation energies calculated for the competitive transition structures in the ***tas*** pathway were found to be more than 1.1 kcal/mol lower in the β-unsubstituted series than in the β-Me-substituted ones.[40] This reduction of the energy gap between the competitive transition structures upon 'hydrogen substitution' conveniently reproduces the lower facial-selectivity reported in the additions to glyceraldehyde derivatives with respect to the β-methyl substituted analogues.[3,5,41] Thus, *trans* substitution at the β-position seems to reinforce the facial bias imposed by the aldehyde α-stereocenter giving rise to a 'fully matched' relationship between the reaction partners.

3.6. Performance of the ONIOM model

To assess the reliability of the particular ONIOM scheme employed in the analysis of the aldol addition we considered the difference between the activation

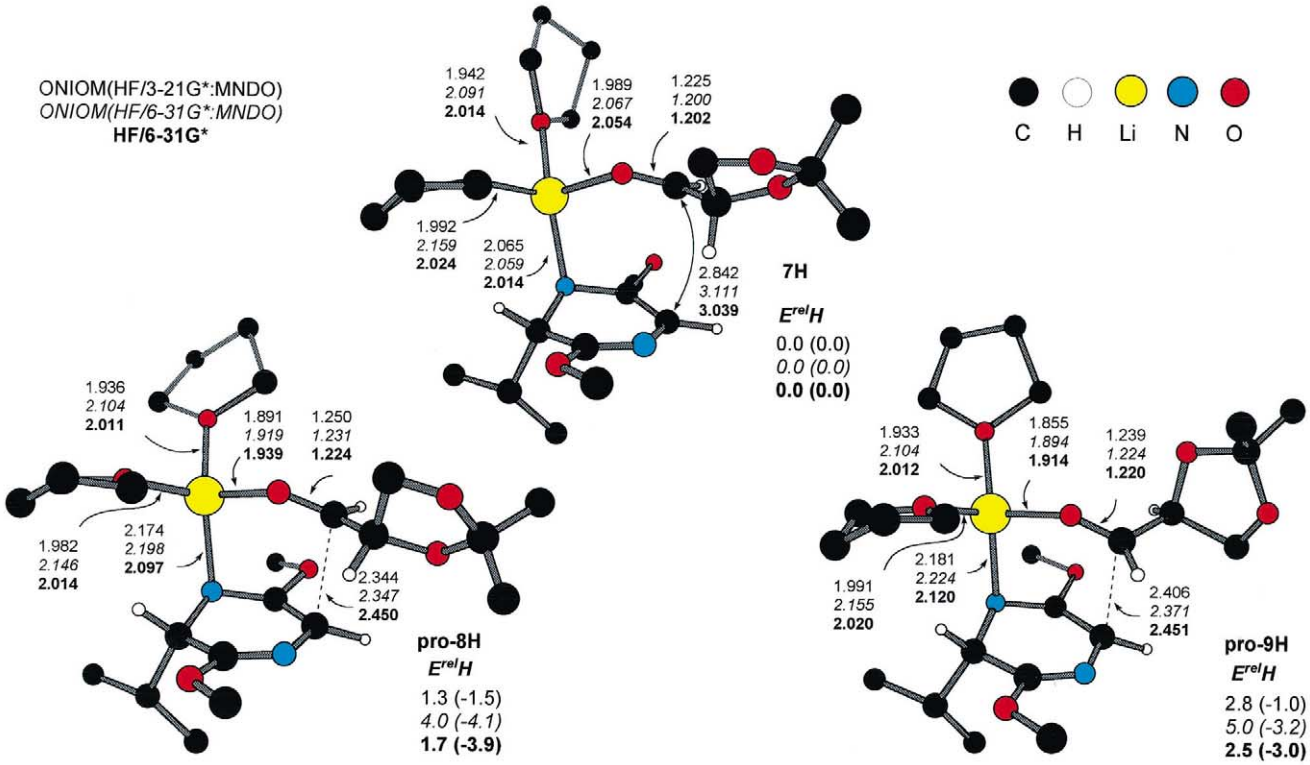

Figure 4. Optimized distances (in Å) and relative energies (in the disolvated reaction channel, $E^{rel}H$) calculated at ONIOM(I) (in plain text), ONIOM(II) (in italics), and HF/6-31G* (in bold) levels for the intermediate complex and the most favored transition structures in the β-unsubstituted series, **7H**, **pro-8H** and **pro-9H**, respectively. Relative single-point energies computed at the B3LYP/6-31+G* level are in parentheses. All energies are in kcal/mol. Hydrogen atoms are omitted, except for the chiral and prochiral centers.

energies of the most stable transition structures in the favored disolvated reaction channel (**pro-8d** and **pro-9d**) as a convenient parameter for the *S*-value test proposed by Morokuma.[42] In this manner the error of the ONIOM(I) and ONIOM(II) extrapolations, with respect to our benchmark calculations at the B3LYP/6-31+G*//HF/6-31G* level, are of 0.86 and 0.60 kcal/mol, respectively. When the geometry optimizations at ONIOM(II) level are followed by single point energy evaluations at the B3LYP/6-31+G* level, the error is reduced to less than 0.10 kcal/mol. Thus, we can conclude that model and method combinations implicit in our ONIOM(I) scheme can be appropriate for the location of the significant stationary points necessary for the rationalization of the stereochemical course of the additions of lithiated bis-lactim ethers to dioxolanecarboxaldehydes. In addition, reoptimization of the significant set of models at the ONIOM(II) level followed by single point energy evaluation at the B3LYP/6-31+G* level can accurately reproduce the results of a complete ab initio calculation with a much lower computational cost.

4. Conclusion

The direction and the relative degree of diastereoselection in the aldol additions of lithiated bis-lactim ethers to dioxolanecarboxaldehydes have been reproduced and rationalized by calculations using pure ab initio (RHF/6-31G*) or two-layer hybrid ab initio:semi-empirical (ONIOM) methods. Thus, six-membered chair-like transition structures with a non-Anh conformation of the aldehyde moiety have been shown to play a dominant role in the aldolate formation. In addition, the β-methyl substituent of the aldehyde, *trans* to the carbonyl group, was found to reinforce the *syn*,*anti* stereoselection of the aldol process by increasing the energy barrier of the competitive pathways.

Model and method combinations implicit in our ONIOM scheme reproduce the results of complete ab initio calculations with lower computational cost, and can result as a valuable computational alternative to intuition and trial and error processes for the analysis of the synthetic applicability of the double stereodifferentiating aldol reactions between metalated bis-lactims and a wide range of α,β-disubstituted aldehydes, particularly in the partially matched situations.

5. Computational details

Calculations reported in this paper were performed using the Gaussian 98 program package[43] on the Athlon workstations of the Aula Net at Facultade de Ciencias of Universidade da Coruña and on the Fujitsu vpp300 at Centro de Supercomputación de Galicia, with the standard 3-21G*, 6-31G* and 6-31+G* basis sets. Some preliminary calculations were performed

using the PC[44] and the Macintosh versions of the GAMESS (US) package.[45] Structures have been fully optimized and characterized by harmonic analysis. All reported reactants, intermediates and products were verified as minima by the absence of negative eigenvalues in the vibrational frequency analysis. For each located transition structure only one imaginary frequency was found in the diagonalized Hessian matrix, and the corresponding vibration was found to be associated with nuclear motion along the reaction coordinate under study. Hybrid calculations were performed with the ONIOM method as implemented in Gaussian 98,[46] using hydrogen atoms as linkers between two layers and default values for the '*f*' parameter, determining the position of the auxiliary hydrogen atoms. ONIOM method does not currently support intrinsic reaction coordinate calculations so the identity of most transition states was confirmed by animating the negative eigenvector coordinate with the GaussView program.[47] For single-point energy calculations including electron correlation at a reasonable computational cost we have used DFT with Becke's three parameter hybrid functional and Lee, Yang, and Parr correlation energies (B3LYP).[48] Zero-point vibrational energies, when computed at the HF/3-21G* and HF/6-31G* were scaled by 0.9409 and 0.9135, respectively.[49]

Conformational space accessible for all the reported models was studied at the ONIOM(RHF/3-21G*:MNDO) level of theory, considering three different rotamers for the isopropyl group of the bis-lactim ether (those with the tertiary carbon atom pointing to the lithium atom, to the nucleophilic carbon atom or to the imidate moiety), two rotamers for each of the methoxy groups (directed to or opposite to the imidate nitrogen) and three rotamers for each of the tetrahydrofuran molecules, thus performing [3×3] and [3×3×3] grid calculations on all the disolvated and three-solvated structures, respectively. A systematic search on the dihedral angles C(2)–N(1)–Li–O(1′), N(1)–Li–O(1′)–C(1′) and Li–O(1′)–C(1′)–C(2′), with a step size of 120°, was also performed for the intermediate complexes **7u**–**d**, starting from geometries with either a *cis* or a *trans* coordination. For the search of transition structures, in all the diastereomeric pathways (***tsa***, ***tas***, ***css*** and ***caa***) of the mono and disolvated reaction channels, three different rotamers (around the O(1′)–C(1′)–C(2′)–O(2′) dihedral angle and characterized by either antiperiplanar, synperiplanar or isoclinal dispositions of the carbonyl and α-alkoxy groups of the aldehyde moiety) were generated with both boat and chair conformations as starting geometries. In the conformational study of the aldolate products **8**–**11**, a search on dihedrals C(2)–C(3)–C(1′)–O(1′) and C(3)–C(1′)–C(2′)–C(3′) was performed with a step size of 120°. Only for the most important conformers located in this search the isopropyl, methoxy and tetrahydrofuran rotamers were also studied.

Acknowledgements

We gratefully acknowledge the Ministerio de Ciencia y Tecnología (BQU2000-0236), the Xunta de Galicia (PGIDT00PXI10305PR), and the Universidade da Coruña for financial support. The authors are indebted to Centro de Supercomputación of Galicia for providing the computer facilities.

References

1. Williams, R. M. In *Synthesis of Optically Active α-Amino Acids*; Baldwin, J. E., Magnus, P. D., Eds.; Organic Chemistry Series, Pergamon: Oxford, 1989; Vol. 7.
2. (a) Bold, G.; Allmendinger, T.; Herold, P.; Moesch, L.; Schär, H.-P.; Duthaler, R. O. *Helv. Chim. Acta* **1992**, *75*, 865–882; (b) Groth, U.; Schöllkopf, U.; Tiller, T. *Tetrahedron* **1991**, *47*, 2835–2842; (c) Gelb, M. H.; Lin, Y.; Pickard, M. A.; Song, Y.; Vederas, J. C. *J. Am. Chem. Soc.* **1990**, *112*, 4932–4942; (d) Schöllkopf, U.; Bardenhagen, J. *Liebigs Ann. Chem.* **1987**, 393–397; (e) Schöllkopf, U.; Nozulak, J.; Grauert, M. *Synthesis* **1985**, 55–56; (f) Schöllkopf, U.; Nozulak, J.; Groth, U. *Tetrahedron* **1984**, *40*, 1409–1417; (g) Schöllkopf, U. *Pure Appl. Chem.* **1983**, *55*, 1799–1806; (h) Schöllkopf, U.; Groth, U.; Gull, M.-R.; Nozulak, J. *Liebigs Ann. Chem.* **1983**, 1133–1151; (i) Schöllkopf, U.; Groth, U.; Hartwig, W. *Liebigs Ann. Chem.* **1981**, 2407–2418.
3. Grauert, M.; Schöllkopf, U. *Liebigs Ann. Chem.* **1985**, 1817–1824.
4. (a) Kobayashi, S.; Furuta, T.; Hayashi, T.; Nishijima, M.; Hanada, K. *J. Am. Chem. Soc.* **1998**, *120*, 908–919; (b) Kobayashi, S.; Furuta, T. *Tetrahedron* **1998**, *54*, 10275–10294; (c) Kobayashi, S.; Matsumura, M.; Furuta, T.; Hayashi, T.; Iwamoto, S. *Synlett* **1997**, 301–303.
5. (a) Ruiz, M.; Ojea, V.; Quintela, J. M. *Tetrahedron: Asymmetry* **2002**, *13*, 1535–1549; (b) Ojea, V.; Ruiz, M.; Quintela, J. M. *Synlett* **1997**, 83–84; (c) Ruiz, M.; Ojea, V.; Quintela, J. M. *Tetrahedron Lett.* **1996**, *37*, 5743–5746.
6. For other highly *syn*,*anti*-selective aldol additions of the stannous salt of Schöllkopf's bis-lactim ethers, see: (a) Ruiz, M; Ojea, V.; Ruanova, T. M.; Quintela, J. M. *Tetrahedron: Asymmetry* **2002**, *13*, 795–799; (b) Ruiz, M; Ojea, V.; Ruanova, T. M.; Quintela, J. M. *Tetrahedron Lett.* **1999**, *40*, 2021–2024; (c) Ruiz, M; Ojea, V.; Quintela, J. M. *Synlett* **1999**, 204–206.
7. Zimmerman, H. E.; Traxler, M. D. *J. Am. Chem. Soc.* **1957**, *79*, 1920–1923.
8. (a) Lodge, E. P.; Heathcock, C. H. *J. Am. Chem. Soc.* **1987**, *109*, 3353–3361; (b) Anh, N. T. *Top. Curr. Chem.* **1980**, *88*, 145–162; (c) Anh, N. T.; Eisenstein, O. *Nouv. J. Chim.* **1977**, *1*, 61–70; (d) Chérest, M.; Felkin, H.; Prudent, N. *Tetrahedron Lett.* **1968**, 2199–2204.
9. Roush, W. R. *J. Org. Chem.* **1991**, *56*, 4151–4157.
10. The term 'non-Anh' transition state has been coined by Heathcock. See Ref. 8a for its definition.
11. Aldol additions of lithium enolates: (a) Abu-Hasanayn, F.; Streitwieser, A. *J. Org. Chem.* **1998**, *63*, 2954–2960; (b) Bernardi, F.; Bongini, A.; Cainelli, G.; Robb, M. A.; Suzzi Valli, G. *J. Org. Chem.* **1993**, *58*, 750–755; (c) Leung-Tong, R.; Tidwell, T. T. *J. Am. Chem. Soc.* **1990**, *112*, 1042–1048; (d) Li, Y.; Paddon-Row, M. N.; Houk, K. N. *J. Org. Chem.* **1990**, *55*, 481–493 and references cited therein.

12. Aldol additions of boron enolates: (a) Bernardi, A.; Gennari, C.; Goodman, J. M.; Paterson, I. *Tetrahedron: Asymmetry* **1995**, *6*, 2613–2636 and references cited therein; (b) Bernardi, F.; Robb, M. A.; Suzzi Valli, G.; Tagliavini, E.; Trombini, C.; Umani-Ronchi, A. *J. Org. Chem.* **1991**, *56*, 6472–6475.
13. Aldol addition of tin(IV) enolates: Yasuda, M.; Chiba, K.; Baba, A. *J. Am. Chem. Soc.* **2000**, *122*, 7549–7555.
14. Aldol additions of lithium azaenolates: Glaser, R.; Hadad, C.; Wiberg, K. B.; Streitwieser, A. *J. Org. Chem.* **1991**, *56*, 6612–6624 and 6625–6637.
15. Aldol additions of boron azaenolates: Bernardi, A.; Gennari, C.; Goodman, J. M.; Leue, V.; Paterson, I. *Tetrahedron* **1995**, *51*, 4853–4866.
16. Amine-catalyzed aldol additions: Bahmanyar, S.; Houk, K. N. *J. Am. Chem. Soc.* **2001**, *123*, 11273–11283.
17. Aldol additions of enols: Bouillon, J.-P.; Portella, C.; Bouquant, J.; Humbel, S. *J. Org. Chem.* **2000**, *65*, 5823–5830.
18. Aldol additions of enoxysilanes: Denmark, S. E.; Griedel, B. D.; Coe, D. M.; Schnute, M. E. *J. Am. Chem. Soc.* **1994**, *116*, 7026–7043.
19. Abbotto, A.; Streitwieser, A.; Schleyer, P. v. R. *J. Am. Chem. Soc.* **1997**, *119*, 11255–11268.
20. Although the X-ray structure of a lithiated bis-lactim ether (derived from *cyclo*-[Ala-Ala]) has been determined as a trisolvated dimeric aggregate, freezing-point depression measurements have shown an average degree of aggregation of 1.15 for the same compound at low temperature diluted ethereal solutions, see: (a) Seebach, D.; Bauer, W.; Hansen, J.; Laube, T.; Schweizer, W. B.; Dunitz, J. D. *J. Chem. Soc., Chem. Commun.* **1984**, 853–854; (b) Bauer, W.; Seebach, D. *Helv. Chim. Acta* **1984**, *67*, 1972–1988.
21. The microsolvation approach has been successfully used for the theoretical study of numerous other solvated lithium compounds, see: Mogali, S.; Daville, K.; Pratt, L. M. *J. Org. Chem.* **2001**, *66*, 2368–2373 and references cited therein.
22. Hehre, W. J.; Radom, L.; Schleyer, P. v. R.; Pople, J. A. *Ab Initio Molecular Orbital Theory*; Wiley: New York, 1986.
23. Parr, R. G.; Yang, W. *Density-Functional Theory of Atoms and Molecules*; Oxford: New York, 1989.
24. Sapse, A.-M.; Schleyer, P. v. R. *Lithium Chemistry: A Theoretical and Experimental Overview*; Wiley: New York, 1995.
25. Svensson, M.; Humbel, S.; Froese, R. D. J.; Matsubara, T.; Sieber, S.; Morokuma, K. *J. Phys. Chem.* **1996**, *100*, 19357–19363.
26. For recent applications of the ONIOM method, see: (a) Lewandowicz, A.; Rudzinski, J.; Tronstad, L.; Widersten, M.; Ryberg, P.; Matsson, O.; Paneth, P.*J. Am. Chem. Soc.* **2001**, *123*, 4550–4555; (b) Feldgus, S.; Landis, C. R. *J. Am. Chem. Soc.* **2000**, *122*, 12714–12727; (c) Bruice, T. C.; Kahn, K. *J. Am. Chem. Soc.* **2000**, *122*, 46–51.
27. Large organic systems have already been studied combining HF and semi-empirical methods for the treatment of the high and low layers within the ONIOM scheme, see: Goldfuss, B.; Rominger, F. *Tetrahedron* **2000**, *56*, 881–884.
28. See Ref. 22, pp. 76–87.
29. Ethyl groups in the bis-lactim ether **3** were replaced by methyl groups to remove additional degrees of conformational freedom in the models **3u–t**. This replacement is expected to result in no significant errors in comparisons between experiment and computations.
30. Dewar, M. J. S.; Thiel, W. *J. Am. Chem. Soc.* **1977**, *99*, 4899–4907.
31. (a) Pratt, L. M.; Kahn, I. M. *J. Comp. Chem.* **1995**, *16*, 1067–1080; (b) Romesberg, F. E.; Collum, D. B. *J. Am. Chem. Soc.* **1992**, *114*, 2112–2121; (c) Kaufman, E.; Raghavachari, K.; Reed, A. E.; Schleyer, P. v. R. *Organometallics* **1988**, *7*, 1597–1607; (d) Glaser, R.; Streitwieser, A. *J. Mol. Struct. (THEOCHEM)* **1988**, *163*, 19–50.
32. Kaufmann, E; Gose, J.; Schleyer, P. v. R. *Organometallics* **1989**, *8*, 2577–2584.
33. Romesberg, F. E.; Collum, D. B. *J. Am. Chem. Soc.* **1995**, *117*, 2166–2178 and references cited therein.
34. McKee, M. L. *J. Am. Chem. Soc.* **1987**, *109*, 559–565 and references cited therein.
35. Hilmersson, G.; Arvidsson, P. I.; Davidsson, O.; Hakansson, M. *J. Am. Chem. Soc.* **1998**, *120*, 8143–8149.
36. In the solid state a tetrameric sodium pinacolonate solvated by pinacolone also adopts a conformationally favourable arrangement for the aldol addition, see: Williard, P. G.; Carpenter, G. B. *J. Am. Chem. Soc.* **1986**, *108*, 462–468.
37. Nevertheless, at the ONIOM(I) level, lowest energy transition structures found in the monosolvated ***tsa*** and ***tas*** pathways were characterized by a tetrahedral environment for the lithium, due to an additional coordination of the cation with the vicinal methoxy group or with the alkoxy group at α-position of the aldehyde moiety. Neither kinetic nor stereochemical evidence for such α-chelation has been found in the reaction of lithium enolates with α-alkoxy aldehydes in THF, see: (a) Heathcock, C. H.; Young, S. D.; Hagen, J. P.; Pirrung, M. C.; White, C. T.; VanDerveer, D. *J. Org. Chem.* **1980**, *45*, 3846–3856; (b) Das, G.; Thornton, E. R. *J. Am. Chem. Soc.* **1993**, *115*, 1302–1312.
38. (a) Lodge, E. P.; Heathcock, C. H. *J. Am. Chem. Soc.* **1987**, *109*, 2819–2820; (b) Heathcock, C. H.; Flippin, L. A. *J. Am. Chem. Soc.* **1983**, *105*, 1667–1668.
39. Bachrach, S. M.; Streitwieser, A. *J. Am. Chem. Soc.* **1986**, *108*, 3946–3951.
40. Activation energies include zero-point vibrational energy corrections computed at the level of geometry optimization.
41. Roush, W. R.; Adam, M. A.; Walts, A. E.; Harris, D. J. *J. Am. Chem. Soc.* **1986**, *108*, 3422–3434 and references cited therein.
42. Vreven, T.; Morokuma, K. *J. Comput. Chem.* **2000**, *21*, 1419–1432.
43. Gaussian 98, Revision A.9, Frisch, M. J.; Trucks, G. W.; Schlegel, H. B.; Scuseria, G. E.; Robb, M. A.; Cheeseman, J. R.; Zakrzewski, V. G.; Montgomery, Jr., J. A.; Stratmann, R. E.; Burant, J. C.; Dapprich, S.; Millam, J. M.; Daniels, A. D.; Kudin, K. N.; Strain, M. C.; Farkas, O.; Tomasi, J.; Barone, V.; Cossi, M.; Cammi, R.; Mennucci, B.; Pomelli, C.; Adamo, C.; Clifford, S.; Ochterski, J.; Petersson, G. A.; Ayala, P. Y.; Cui, Q.; Morokuma, K.; Malick, D. K.; Rabuck, A. D.; Raghavachari, K.; Foresman, J. B.; Cioslowski, J.; Ortiz, J. V.; Baboul, A.

G.; Stefanov, B. B.; Liu, G.; Liashenko, A.; Piskorz, P.; Komaromi, I.; Gomperts, R.; Martin, R. L.; Fox, D. J.; Keith, T.; Al-Laham, M. A.; Peng, C. Y.; Nanayakkara, A.; Challacombe, M.; Gill, P. M. W.; Johnson, B.; Chen, W.; Wong, M. W.; Andres, J. L.; Gonzalez, C.; Head-Gordon, M.; Replogle, E. S. and Pople, J. A. Gaussian, Inc., Pittsburgh PA, 1998.

44. Alex A. Granovsky, http://classic.chem.msu.su/gran/gamess/index.html.
45. Schmidt, M. W.; Baldridge, K. K.; Boatz, J. A.; Elbert, S. T.; Gordon, M. S.; Jensen, J. H.; Koseki, S.; Matsunaga, N.; Nguyen, K. A.; Su, S. J.; Windus, T. L.; Dupuis, M.; Montgomery, J. A. *J. Comput. Chem.* **1993**, *14*, 1347–1363.
46. Dapprich, S.; Komiromi, I.; Byun, K. S.; Morokuma, K.; Frisch, M. J. *J. Mol. Str. (THEOCHEM)* **1999**, *461–462*, 1–21.
47. GaussView, version 2. Gaussian, Inc. http://www.gaussian.com.
48. Kohn, W.; Becke, A. D.; Parr, R. G. *J. Phys. Chem.* **1996**, *100*, 12974–12980.
49. Pople, J. A.; Scott, A. P.; Wong, M. W.; Radom, L. *Israel J. Chem.* **1993**, *33*, 345–350.